

The Effect of Snow Cover on the Climate

JUDAH COHEN* AND DAVID RIND**

**Department of Geological Sciences, Columbia University, New York, New York*

***NASA/Goddard Space Flight Center, Institute for Space Studies, New York, New York*

(Manuscript received 9 February 1990, in final form 17 December 1990)

ABSTRACT

Large-scale snow cover anomalies are thought to cause significant changes in the diabatic heating of the earth's surface in such a way as to produce substantial local cooling in the surface temperatures. This theory was tested using the GISS 3-D GCM (General Circulation Model). The results of the GCM experiment showed that snow cover caused only a short term local decrease in the surface temperature. In the surface energy budget, reduction in absorbed shortwave radiation and the increased latent heat sink of melting snow contributed to lower temperatures. However, all the remaining heating terms contribute to increasing the net heating over a snow covered surface. The results emphasize the negative feedback which limits the impact of snow cover anomalies over longer time scales.

1. Introduction

Of all the varying surface conditions, snow cover experiences the largest fluctuations, both spatially and temporally. An isolated cyclonic event can increase the continental snow cover on the order of 1000 km. The most recognizable effect of snow cover is the change it forces on the radiation and/or energy budget of the lower atmosphere and the surface, thus potentially playing a role in climatic fluctuations. Since the diabatic heating of the atmosphere provides the forcing for atmospheric motions snow could alter the dynamics of the atmosphere.

Snow is thought to influence local temperatures in several ways:

- 1) The high reflectivity of fresh snow can increase the surface albedo by 30%–50% (see Table 1, taken from Sellers 1965).
- 2) Wagner (1973) has suggested that because snow has a higher thermal emissivity than most other natural surfaces (see Table 2, also taken from Sellers), it tends to increase the amount of infrared radiation lost.
- 3) Fresh snow acts as a thermal insulator because of its low thermal conductivity, preventing a positive flux of sensible heat from the ground into the lowest atmospheric layer.
- 4) Melting snow is a sink for latent heat.

Most studies conducted on the effect of snow cover on surface temperatures have been empirical in nature.

Early studies compared winter temperature anomalies with snow cover variance (Namias 1960, 1962, 1985; Wagner 1973; Dewey 1977). They concluded that surface snow cover depressed temperatures on the order of 5°C over the course of several days to several months.

Walsh et al. (1982) conducted a more general study of snow cover and temperatures over the United States (winters 1950–79). First they correlated the departure from normal temperatures and the departure from normal snow cover. They concluded that colder than normal temperatures are associated with above normal snow cover. Also correlated were snow cover and height anomalies, and it was found that positive snow anomalies are associated with below normal height anomalies, in the eastern United States. Finally snow cover was correlated with antecedent heights and subsequent heights; a stronger signal existed between snow cover and height anomalies for the antecedent heights than for the subsequent heights. This is evidence that the heights (dynamics) force the snow cover rather than vice versa.

The authors compute, through the use of regression analysis, the contribution of snow cover to the variance in temperature. Values computed by the authors were as high as 20% for the whole winter in the midwestern United States. The authors also made calculations for the individual winter months and found that snow as a tool for temperature prediction for the same month tends to increase in accuracy by the end of the winter, suggesting that the influence of snow cover on the localized temperatures increases as the amount of solar radiation that reaches the ground increases and the increased albedo of snow grows in importance. When the average monthly snow cover was calculated as a

Corresponding author address: Judah Cohen, Goddard Institute for Space Studies, 2880 Broadway, New York, NY 10025.

TABLE 1. Chart of albedos (in percent) for shortwave radiation for naturally occurring surfaces (Sellers 1965) (wavelengths $<4.0 \mu$).

<i>A. Water Surfaces</i>	
Winter— 0° lat	6
30° lat	9
60° lat	21
Summer— 0° lat	6
30° lat	6
60° lat	7
<i>B. Bare Areas and Soils</i>	
Snow, fresh fallen	75–95
Snow, several days old	40–70
Ice, sea	30–40
Sand dune, dry	35–45
Sand dune, wet	20–30
Soil, dark	5–15
Soil, moist gray	10–20
Soil, dry clay or gray	20–35
Soil, dry light sand	25–45
Concrete, dry	17–27
Road, black top	5–10
<i>C. Natural Surfaces</i>	
Desert	25–30
Savanna, dry season	25–30
Savanna, wet season	15–20
Chaparral	15–20
Meadows, green	10–20
Forest, deciduous	10–20
Forest, coniferous	5–15
Tundra	15–20
Crops	15–25

predictor of the ensuing months, however, the signal disappeared.

Foster et al. (1982) did an empirical study on the seasonal effects of snow cover for both Eurasia and North America. Their study compares the relationship between 1) continental snow cover as measured in the autumn and the ensuing winter's temperatures, and 2) continental snow cover as measured in the winter and the concurrent winter's temperatures. For Eurasia, the amount of variance for winter temperatures, explained by the autumn snow cover ranges between 18% and 52%; most correlations are significant at the 95% level. For North America, the values are only 4%–12% and the level of significance is generally below the 90% level. For the experiment where winter snow cover was correlated with winter temperatures, the results reversed. For North America the variance in temperature explained by snow cover increased to 46%, while for Eurasia the variance dropped to 4%.

More recent studies have employed more sophisticated statistical approaches, with similar results. Klein (1983, 1985) and Klein and Walsh (1983) devised a method of calculating the probable temperature anomalies from the observed 700 mb circulation using empirical orthogonal functions (EOFs). Researchers later used Klein's methods to try to separate out from the temperature data, how much of the temperature is a function of the 700 mb circulation and how much

is a function of other variables. Therefore, if a station has snow cover, its probable temperature, calculated from the circulation, can be subtracted from the observed temperatures, and the difference is presumably due to the snow cover itself.

Walsh et al. (1985) did such a study for the United States during the winter months (1947–80). The authors calculated surface temperature predictions from the 700 mb height field for both heavy and light snow cover. They then subtracted the predictions from the observed temperatures and attributed the error to varying snow cover. In cases where there was heavy snow cover the error tended to be more negative than for light snow cover by as much as 2.0°C . Therefore the authors conclude that snow cover suppresses air temperatures. Once again the authors found that the amount the temperature is suppressed increases as the winter progresses.

The most recent studies on the effects of snow cover have been model studies; however the emphasis has been on dynamics rather than thermodynamics. Walsh and Ross (1986, 1988) devised a model experiment using the NCAR (National Center for Atmospheric Research) CFM (Community Forecast Model) to see how snow and ice cover influence the synoptic features of the atmosphere. This is complicated because snow cover influences the circulation in a nonlinear fashion. Walsh and Ross (1986) tried to isolate the influence of snow cover and sea ice on the development of cy-

TABLE 2. Chart of thermal emissivities (percent) for naturally occurring surfaces (Sellers 1965).

<i>A. Water and Soil Surfaces</i>	
Water	92–96
Snow, fresh fallen.	82–99.5
Snow, ice granules	89
Ice	96
Soil, frozen	93–94
Sand, dry playa	84
Sand, dry light	89–90
Sand, wet	95
Gravel, corase	91–92
Limestone, light gray	91–92
Concrete, dry	71–88
Ground, moist, bare	95–98
Ground, dry plowed	90
<i>B. Natural Surfaces</i>	
Desert	90–91
Grass, high dry	90
Fields and shrubs	90
Oak woodland	90
Pine forest	90
<i>C. Vegetation</i>	
Alfalfa, dark green	95
Oak leaves	91–95
Leaves and plants	
0.8 μ	5–53
1.0 μ	5–60
2.4 μ	70–97
10.0 μ	97–98

clonic systems using various short range forecasts and comparing them to the observed fields. They concluded that heavy snow cover causes lower geopotential heights and lower sea level pressures (as much as 11 mb) along the east coast of North America. Nothing was mentioned about surface temperatures.

Walsh and Ross (1988) found similar results for 30 day model runs, i.e., higher snow cover produces lower sea level pressure along the east coasts of North America and Asia. The authors did look at temperatures and found near-surface temperatures to be colder locally by as much as 5°–10°C when greater snow cover is prescribed in the model run.

Barnett et al. (1988, 1989) conducted modeling studies on varying snow cover in the GCM (General Circulation Model) from ECMWF (European Centre for Medium Range Weather Forecasts). These studies have mostly concentrated on global teleconnections rather than local surface temperatures. However, it was found that even though in an above normal snow cover situation the higher albedo causes a net heat loss, more energy is gained through the latent heating term and there is actually a net heat gain. This net heat gain causes an increase in snow melt which results in an overall net heat loss and thus a negative temperature anomaly.

Finally Peterson and Hoke (1989) looked at the dependence of forecasts made from the Nested Grid Model (NGM) on the snow cover analysis. They found that using a snow cover analysis done on 18 January 1988 for a 24 January 1988 forecast caused the NGM to underpredict temperatures by 10°C for the Washington, D.C., area. The reason for this discrepancy was that snow cover was present in the Washington, D.C., area on 18 January 1988, and therefore included in the snow cover analysis, but had melted by the forecast period. When Petersen and Hoke reran the NGM, with the snow cover removed from the Washington, D.C., area, predicted temperatures were as much as 7°C warmer than the original forecast.

Empirical studies are difficult to interpret since snow cover, temperatures and the atmospheric circulation are all interdependent. Any signal found from these studies is subject to ambiguity due to the complex dynamics of the atmosphere. Therefore, for any study to be valid it must use an objective method in separating the cooling due to snow cover from cooling due to all other effects. Several studies have attempted to overcome this difficulty using a procedure for specifying surface temperatures as a function of midtropospheric height patterns; however the procedure is not unique, as the same height can be generated by varying temperature profiles (e.g., colder at the surface and warmer in the midtroposphere, or the reverse). The question which is difficult to resolve from empirical studies is: if a winter with higher snow cover is colder than normal, is it colder because of the snow cover, or is there more snow because it is colder? In this paper the goal

is to separate these effects by altering the snow cover directly, and utilizing modeling experiments to evaluate the effects of snow cover on the local temperature and energy balance of the atmosphere near the surface.

2. Model experiment

The experiment was carried out using the Goddard Institute for Space Studies (GISS) 3-D GCM (Hansen et al. 1983). In this model the primitive equations are solved on a grid point domain with 8° latitude by 10° longitude horizontal resolution and nine layers in the vertical, with a top layer at 10 mb. For each grid box fundamental physical quantities are calculated, such as heat and moisture transport through a two-layer ground, surface hydrological properties and albedo as a function of vegetation type, complete radiative cloud calculations, diurnal cycle, etc.

Fractional grid types are used, so that each grid box may contain land, ocean, sea ice or land ice. Snow may accumulate on land, land ice or sea ice. The sea surface temperature and sea ice were specified in the model from the monthly climatologies of the ocean dataset of Robinson and Bauer (1981). Values are given for the middle of the month and are interpolated daily. Were these quantities allowed to change it would add to the model's variability, but considering the short duration of the run, this would not noticeably change the results.

The model was initiated using the initial atmospheric conditions of December 1977, and the model run was carried out for five years. The experiments for this paper were conducted for the month of March of each model year (1978–1982). Each individual March was run with the initial conditions as generated by the model, with the exception of snow cover which was prescribed. Thus, for each March model run the synoptic situation varies from year to year while the initial snow cover remains the same.

Snowfall occurs in the GISS GCM whenever there is precipitation and the surface temperature is at or below freezing in the lowest model layer. Snow melt can only occur at 0°C; once the air temperature in the model reaches 0°C and snow cover is present, any additional heating goes into melting the snow while the temperature remains at 0°C. Only once all the snow is melted will the temperature go above 0°C. Snowfall occurs at the rate of 1 cm/1 mm of melted equivalent water. Fresh snow is prescribed an albedo depending on the snow depth and vegetation cover; in addition, the albedo decreases as a function of age [refer to Hansen et al. (1983) and Rind et al. (1989) for a more complete discussion].

Data for the frequency of snow cover were obtained from the NOAA Atlas of Satellite-derived Northern Hemispheric Snow Cover Frequency (Matson et al. 1986). For the month of March, the 50% frequency of snow cover contour of the Matson et al. dataset gen-

erally lies within a few degrees of 45°N. In comparison, the 50% snow coverage in the model (averaged for all land points) lies slightly north of 43°N on 1 March. The model generated snow cover and observations agree favorably and data from the observations can be used successfully as model input. The snow cover frequency dataset was used to prescribe two runs for each March: 1) a “maximum” snow cover run, where on 1 March, snow is present inside any grid box that has a snow cover frequency greater than one percent for the month of March (see Fig. 1); 2) a “minimum” snow cover run, where on 1 March, snow is present only in those grid boxes that have a 100% frequency of snow cover for the month of March (see Fig. 1). Snow depths for each grid box were taken from the GCM control run, and in those boxes where the GCM did not produce any snow a depth of 1 kg m⁻² (= 1 cm) was prescribed.

It should be noted that most of the results and discussion presented in the paper are based on those grid boxes where the model had already produced a preexisting snow cover (the only exception being western Europe) on 1 March. Therefore, no changes were necessary for the maximum snow cover run in those grid boxes. In order to make the minimum snow cover run, the snow cover had to be removed from those grid boxes. This could lead to an underestimate of the impact of snow cover since the model might put back snow cover in the minimum snow cover run; however, significantly less snow cover remained in the minimum snow cover run throughout the remainder of the month during the experiment.

An alternate problem could arise using the month of March: if snow cover was removed too rapidly in the maximum snow cover run, it could minimize the snow cover impact. For example, had the results of the experiment been derived from regions where snow was added to grid boxes where the model did not want snow, this would have tended to underestimate the impact of snow cover by removing it too rapidly. However, the snow cover in the maximum snow cover run was sufficiently deep to remain for most of the month. At 51°N, the latitude at which most of the model results were derived, the averaged snow cover for all five months of March was 67%, indicating a stable, durable snow cover despite it being late winter.

3. Results

The initial results relevant to the discussion of the paper are presented in Figs. 2–4. The differences between the two model runs in the five-year monthly means for the month of March of the following quantities are plotted: ground albedo, composite surface air temperature, and the composite net absorbed solar radiation at the surface.

a. Albedo

The values obtained for the differences in the ground albedo between the maximum snow cover run and the minimum snow cover run are presented in Fig. 2. Using the values obtained and assuming that the most important aspect of snow cover which affects local temperatures is its high albedo, a first-order approximation for the temperature change due to an anomalous snow cover can be derived by using a zero-dimensional energy balance, where outgoing and incoming radiation balance:

$$\sigma T^4 = (1 - \alpha)S_0$$

taking finite differences, setting T equal to T_0 (surface temperature) and rearranging:

$$\Delta T = \frac{-S_0 \Delta \alpha}{4\sigma T_0^3}, \quad (1)$$

where σ is the Stefan–Boltzman constant, S_0 is the solar radiation incident on the surface and α is the ground albedo. For example, at 51°N latitude, using values of $\Delta \alpha = 24\%$, $S_0 = 114 \text{ W m}^{-2}$, and $T_0 = 270 \text{ K}$, ΔT is approximately equal to minus 6°C. This value of ΔT includes only the change in albedo. Looking at the temperature differences between the two runs, we see that there are only small differences in the surface air temperature between the two runs for the monthly averages (see Fig. 3). Most temperature differences are equal to or less than 3°C (within one standard deviation), the only exception being a small region in central Asia, where the temperature difference reaches a value of –5.5°C, a difference of two standard deviations.

The small temperature difference between the maximum and the minimum snow cover runs is even more surprising when looking at the net solar radiation absorbed at the surface (Fig. 4). Values of ΔS_{abs} (difference in the absorbed shortwave radiation at the ground) are on the order of 10–20 W m⁻². This is a large enough energy deficit to cause a temperature difference on the order of 10°C, based upon the amount of energy absorbed at the earth’s surface and the resultant surface temperature. A more comprehensive understanding of the whole energy budget is required in order to explain the minimal monthly averaged temperature difference between the two model runs.

b. Energy balance

The averaged temperature differences between the first ground layer and the surface air temperatures are all within 1°C. Since the energy balance at the ground is straightforward and readily available from the computer diagnostics, the energy balance of the first ground layer will be discussed rather than the energy balance of the atmosphere.

The energy balance of the first ground layer is

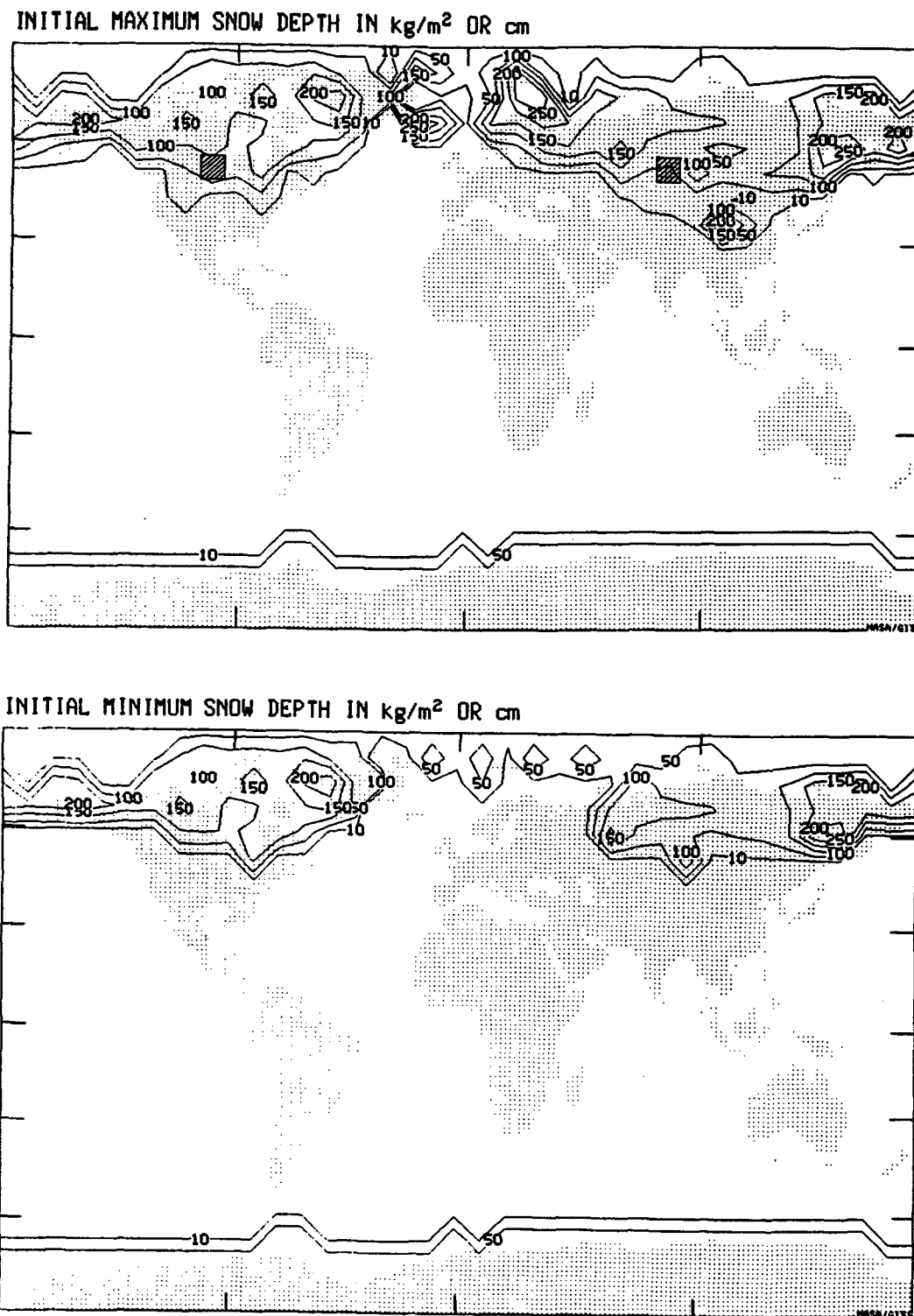


FIG. 1. The initial snow depth (in kg m^{-2}) on 1 March, for all the model years (1978–82) for (a) the maximum snow cover run and (b) the minimum snow cover run. The snow cover was not varied from year to year. Also drawn, using diagonal lines, are the grid boxes centered at 51°N , 70°E and 51°N , 100°W . Tick marks indicate the equator, 30° and 60° N and S, the Greenwich meridian and 90° E and W. For the purpose of figure clarity, an irregular contour interval was prescribed—10, 50, 100, 150, 200, 250 and 300 cm intervals was used.

GROUND ALBEDO (PERCENT) FIVE YEAR MONTHLY MEAN MAX-MIN SNWCVR

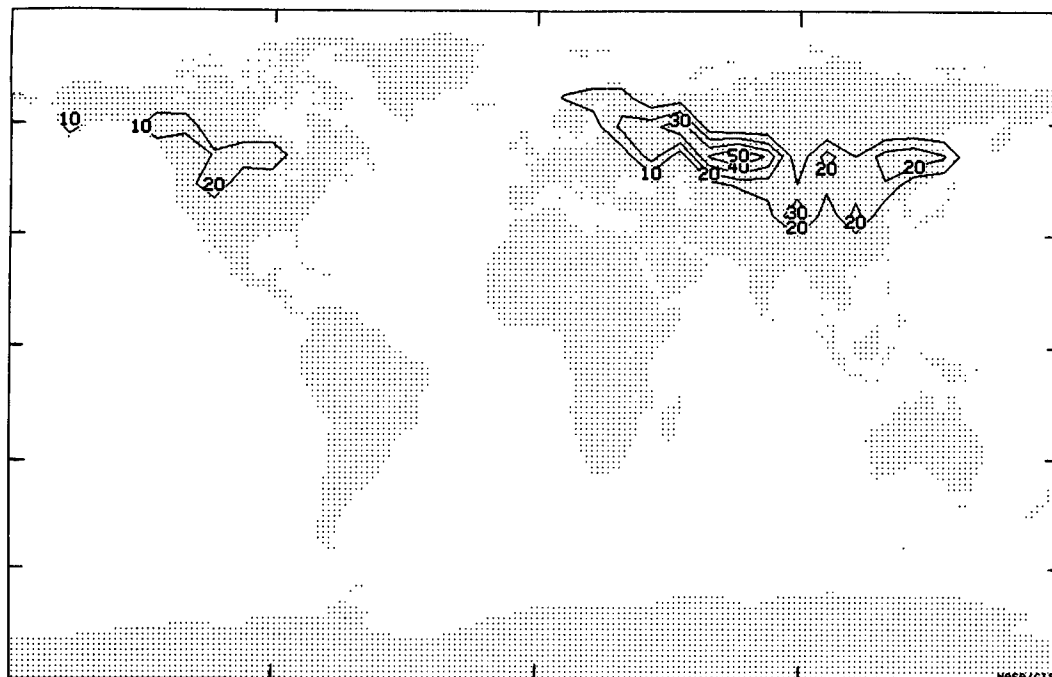


FIG. 2. The five-year monthly averaged ground albedo for the maximum snow cover run minus the five-year monthly averaged ground albedo for the minimum snow cover run. (Henceforth all differences are to be understood as the maximum snow cover run minus the minimum snow cover run.) Notice that the largest differences are found in central Asia.

COMPOSITE SURF AIR TEMP (C) FIVE YEAR MONTHLY MEAN MAX-MIN

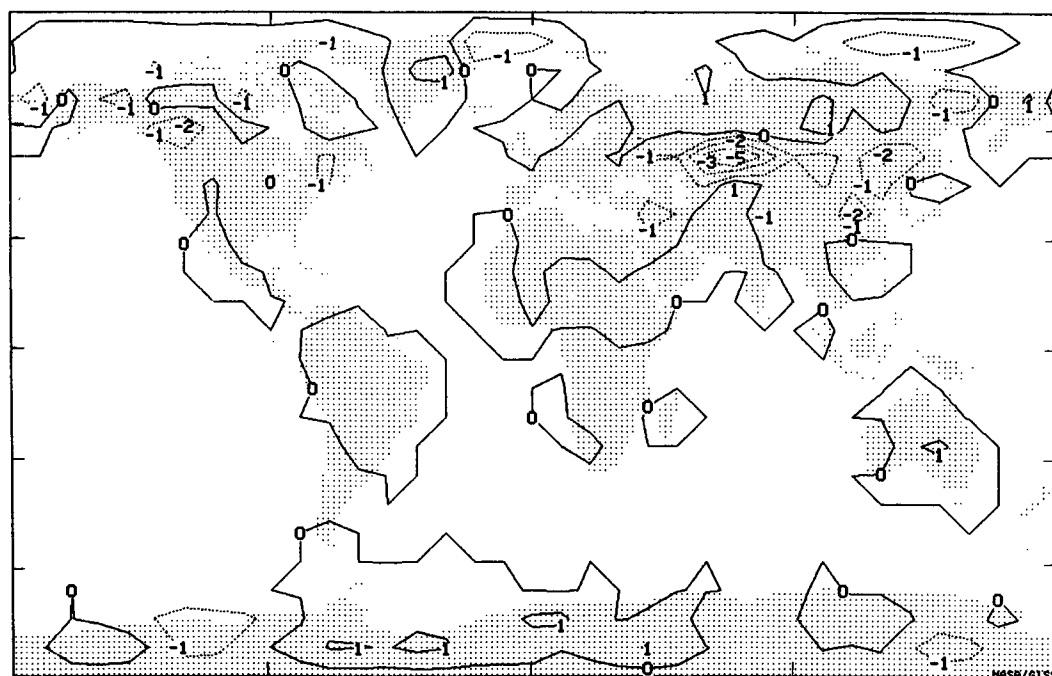


FIG. 3. The difference in the five-year monthly averaged surface air temperature. Negative contours are dashed and positive contours are solid. Note again that the largest differences exist in central Asia.

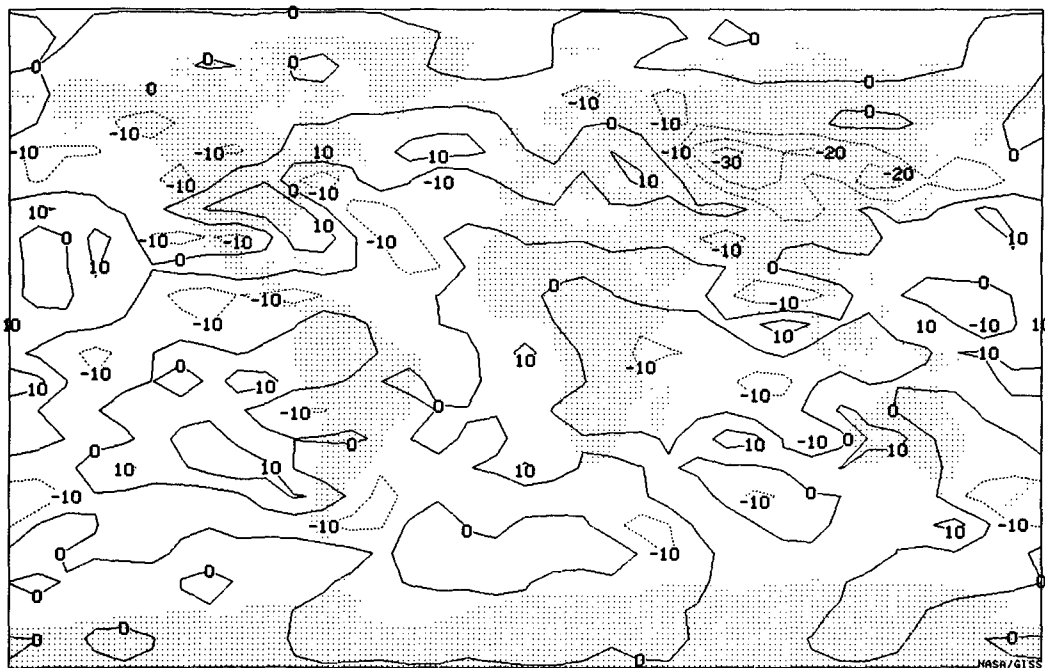
NET SOLAR RADIATION AT SURFACE (Wm^{-2}) 5 YR MNTHLY MEAN MAX-MIN

FIG. 4. The difference in the five-year monthly averaged absorbed solar radiation.

$$\Delta E = SW - LW - SH - LH + DIF + PREC,$$

where

- ΔE the net change in energy
 SW the net gain in shortwave radiation
 LW the net loss in longwave radiation
 SH the net loss in energy due to sensible heat fluxes
 LH the net loss in energy due to latent heat fluxes
 DIF the net gain/loss of energy due to diffusion from the second ground layer
 PREC the net gain/loss of energy due to the temperature difference between the ground and the precipitation.

The last two terms are not discussed further since they are small and equal for both runs.

Given that the temperature difference between the two model runs for any individual grid point is within one standard deviation, and the relatively small time scale of the GCM run, the significance of the results should be enhanced by averaging over many grid points. Therefore, we discuss the energy balance averaged over land for 8° -wide latitude bands, in particular the band centered at 51°N . This latitude was chosen due to the nature of the experiment, the largest differences in the snow cover are realized at 51°N , and there is a relatively large percentage of land present at this latitude.

Table 3 gives a list of the respective values for each energy term at 51°N , for the two runs. Also shown in

Table 3, are the same energy terms at 59°N , for comparison. Given in Table 4 are the standard deviations for the energy terms at both latitudes, and it is readily

TABLE 3. The latitudinally, five-year-averaged energy terms (W m^{-2}) for both the maximum snow cover run for (a) 51°N and (b) 59°N . Also included are the net heating term and temperature of the model's first ground layer. In the energy terms, net downward energy is positive and net upward energy is negative. Also all energy terms are rounded off in the tables.

Energy term	Maximum	Minimum
(a) Snow cover at 51°N		
Shortwave radiation	80	88
Longwave radiation	-32	-33
Sensible heat flux	-13	-17
Latent heat flux	-28	-33
Precipitation heat flux	-5	-4
Net heating	3	1
Snow cover (kg m^{-2})	42	9
Ground temperature ($^\circ\text{C}$)	-3.9	-3.2
(b) Snow cover at 59°N		
Shortwave radiation	60	63
Longwave radiation	-31	-32
Sensible heat flux	-9	-11
Latent heat flux	-14	-17
Precipitation heat flux	-4	-5
Net heating	1	-1
Snow cover (kg m^{-2})	97	65
Ground temperature ($^\circ\text{C}$)	-8.7	-8.7

TABLE 4. Standard deviations for all the terms listed in Table 3.

	59°N	51°N
Shortwave radiation	2.6	2
Longwave radiation	1.8	1
Sensible heat flux	1.3	1.5
Latent heat flux	0.5	0.7
Precipitation heat flux	0.4	0.2
Net heating	0.7	0.7
Ground temperature (°C)	1.04	0.71

seen that the difference between the individual energy terms between the two runs is greater than two standard deviations (with the exception of the emitted longwave radiation). Yet, the resultant temperature difference at 51°N is only on the order of one standard deviation, the same result that was obtained from looking at the individual grid points. The only energy term less in value in the maximum snow cover run than in the minimum snow cover run is the shortwave radiation absorbed at the ground. Contrary to the reasoning given in the Introduction implying that snow cover should increase the net energy loss at the surface, the energy difference between the two runs shows a net gain of energy at 51°N for the maximum snow cover run! The same result applies at 59°N. We now discuss the individual terms separately.

c. Shortwave radiation

The large changes observed in the ground albedo are consistent with theory. However, the changes in the surface temperatures and the absorbed solar radiation do not reflect the large changes in ground albedo. For example, at 51°N the change in the ground albedo was more than 20% (absolute) greater in the maximum snow cover run compared to the minimum snow cover run, yet the temperature change was only 0.7°C. It is not the ground albedo that ultimately affects the absorbed shortwave radiation but rather the planetary albedo. At 51°N the absolute difference in the planetary albedo between the two runs is only 2%, i.e., the planetary albedo is 2% higher in the maximum snow cover case than in the minimum snow cover case. The large discrepancy between the change in the ground albedo and the planetary albedo is due partly to cloud cover changes that offset the importance of the ground albedo change, and partly due to the fact that shortwave radiation, both direct and reflected off the snow cover, is absorbed to some degree by the atmosphere and re-radiated back down to the surface.

In all the GCM experiments clouds were computed and not prescribed, which enables the snow cover to interact with the cloud cover. Large-scale cloud cover is computed as the saturated fraction of the grid box under the assumption that the absolute humidity is

uniform throughout the grid box and temperature has subgrid-scale variation. Convective clouds are produced in a grid box where in the mean, the grid box is conditionally unstable. For more details please refer to Hansen et al. (1983).

Rossow and Lacis (1990) compared cloud data to clouds in the GISS GCM and found the GCM to be in good agreement with data and climatology. Computed differences between data and the climate GCM calculations are on the same order of magnitude as the uncertainties in the data analysis and its differences with available validation. Therefore, it is assumed that to first order the clouds in the GCM respond in a realistic manner to the snow cover.

In the maximum snow cover run, cloud cover decreased by 2% (a change of four standard deviations) when compared to the minimum snow cover run, as did the atmospheric albedo, a result of increased subsidence above the colder surface. Another likely contributing factor to fewer low clouds above the snow covered surface is a surface moisture–evaporation–cloud feedback process noted in Meehl and Washington (1988). The more evaporation from the surface, the more moisture in the atmosphere and therefore the more clouds. As will be shown later (Table 3), latent heat flux is diminished over a snow covered ground, which is an indication of less surface evaporation when snow is present. Less surface evaporation dries out the atmosphere and decreases cloud cover. The decrease in cloud cover lessens the difference in the planetary albedo between the two runs. In addition, some 10% of the total incoming shortwave radiation is absorbed in the atmosphere and cannot be affected by changes in the ground albedo. At 51°N the difference in the absorbed solar radiation at the surface is 8 W m^{-2} or about 3% of the total incoming solar radiation (still a significant amount), almost the same as the change in planetary albedo and only a tenth of the change in the ground albedo.

The presence of cloud cover determines how effective the ground albedo change can be in altering the absolute amount of radiation at the surface. In regions where cloud cover is sparse the ground albedo can have a much larger impact on the absorbed solar radiation. For example in western Siberia, the difference in the ground albedo is about 25%, or one-quarter more than the latitudinal average, and the change in planetary albedo is 10%, five times greater than the latitudinal average. In this region with little cloud cover, solar radiation easily reaches the ground, so the ground albedo can have a larger impact on the overall energy balance. The difference between the two runs in the absorbed solar radiation is 25 W m^{-2} (10% of the overall incoming solar radiation), three times greater than in the latitudinal average. A change of this magnitude in the overall energy balance can have a large impact on the surface temperatures.

d. Longwave radiation

The small net increase in outgoing longwave radiation in the minimum snow cover run indicates that the higher emissivity of snow is insignificant. Rather, the lower temperatures at the ground in the maximum snow cover run inhibit the amount of outgoing radiation emitted by the surface. Since temperature dominates the emitted longwave energy term, less energy is emitted in the snow cover case, not more.

e. Sensible and latent heat

The latitudinally averaged loss of energy due to the sensible and latent heat terms increased from the maximum snow cover run to the minimum snow cover run, for both latitudes shown in Table 3. For a more detailed examination of the sensible and latent heat terms, it is necessary to look at certain individual grid boxes. Two grid boxes were chosen:

1) 51°N, 70°E: geographically located in the Central Soviet Union, and

2) 51°N, 100°W: geographically located in the midwest of Canada (the corresponding grid boxes for these two locations are indicated in Fig. 1 by the diagonal lines).

These points were chosen because they are situated in continental regions. Such regions are far from ocean influences and where the climate is dominated by high pressure, less cloud cover and light winds. In such regions snow cover is most likely to have the greatest impact on the energy balance.

The sensible and latent heat fluxes, from the ground into the surface air layer, are computed in the model using a drag law parameterization (Deardoff 1967),

$$F_h = C_p \rho C_h V_s (T_g - T_s), \quad (2)$$

$$F_q = \beta \rho C_q V_s (q_g - q_s), \quad (3)$$

where

F_h the sensible heat flux from the ground to the surface air layer

F_q the latent heat flux from the ground to the surface air layer

ρ the density of air

C_p specific heat of air

C_h heat transfer coefficient

V_s surface wind (vector quantity)

T_g ground temperature

T_s surface air temperature

β an efficiency factor

C_q humidity transfer coefficient

q_g water vapor mixing ratio of the ground

q_s water vapor mixing ratio of the surface air layer.

The transfer coefficients are computed using the Rich-

ardson number, Ri , and a drag coefficient, C_D . (For a more detailed discussion refer to Hansen et al. 1983).

For non-neutral stability,

$$C_q = C_h = 1.35 \left[\frac{(1 - d Ri_s)}{(1 - f Ri_s)} \right]^{1/2}, \quad (4)$$

where

Ri_s the bulk Richardson number for the surface air layer, i.e.,

$$Ri_s = \frac{z_s g (T_s - T_g)}{T_g V_s^2}, \quad (5)$$

z_s the height of the surface air layer (prescribed equal to 30 m over land surfaces)

g the acceleration due to gravity

(d and f are coefficients for the transfer coefficients equation as a function of $\log_{10}(z_s/z_0)$, where z_0 is the surface roughness).

From Eqs. (2)–(5) the sensible and latent heat fluxes are dependent on the vertical temperature profile and the square of the magnitude of the surface wind speed. Little or no difference in the surface wind speeds between the model runs was found at these grid points when averaged over the whole month. Therefore, the difference between the two runs in the sensible and latent heat flux terms must be only a function of the vertical temperature profile.

Table 5 compares the change in potential temper-

TABLE 5. The important parameters affecting the sensible and latent heat flux away from the model surface. The table includes the five-year monthly averaged: change in potential temperature between the surface air layer and the ground layer in degrees kelvin, the Richardson number for that layer multiplied by 10^2 , the heat transfer coefficient multiplied by 10^4 , and the combined value of the sensible and latent heat flux at the ground for (a) 0800 UTC (noon local time) for western Siberia and (b) 1900 UTC (noon local time) for central Canada. Shown are the individual numbers for both the maximum snow cover run and the minimum snow cover run.

	Snow cover	
	Maximum	Minimum
(a) Western Siberia		
$T_{\text{surface air}} - T_{\text{ground}}$ (K)	-1.2	-1.8
Richardson number at ground		
surface	-13.4	-16.8
C_h ($\text{W m}^{-2} \text{ } ^\circ\text{K}^{-1}$)	127.6	139.4
Sensible + latent heat (W m^{-2})	-142.4	-218.4
(b) Central Canada		
$T_{\text{surface air}} - T_{\text{ground}}$ (K)	-1.8	-2
Richardson number at ground-		
surface	-5.8	-7.2
C_h ($\text{W m}^{-2} \text{ } ^\circ\text{K}^{-1}$)	97.2	104.2
Sensible + latent heat (W m^{-2})	-101.8	-179.6

ature between the ground and the surface air layer. The slope of the potential temperature is an indication of how stable the atmosphere is to convection and turbulence. Table 5a lists the change in potential temperature in the lowest layer of the model atmosphere for the central Soviet Union and Table 5b lists the same values for midwestern Canada. Each table is for noon local time, a time at which the atmosphere can best support turbulence and convection.

Both tables demonstrate that the vertical temperature profile in the minimum snow cover run is more unstable (indicated by the larger negative slope) in the lowest layers of the atmosphere than in the corresponding atmosphere of the maximum snow cover run. The lower atmosphere in the minimum snow cover run becomes slightly more unstable during the most intensive heating of the day. The greater instability is further reflected in the Richardson number (also listed in Table 5), as the temperature profile acquires a more negative slope the Richardson number achieves higher negative values [Eq. (5)]. In turn, the drag coefficient, which is a function of the Richardson number and is always positive, becomes larger in value [Eq. (4)], as is indicated in Table 5. The final result is that larger values of sensible and latent heat fluxes occur in the minimum snow cover run.

Figure 5 demonstrates how the value of the drag coefficient increases greatly with decreasing values of the Richardson number. As the Richardson number approaches zero, small differences can result in large differences in the magnitude of the drag coefficient, which in turn increases the amount of energy flux away from the surface. Therefore, the lower Richardson numbers attained in the minimum snow cover run

would allow for substantially more sensible and latent heat to be transported away from the surface than in the maximum snow cover run. This result is best demonstrated in the values of C_h , the heat transfer coefficient, which is directly proportional to the drag coefficient [Eq. (4)]. Figure 6 compares the hourly monthly averaged values of the heat transfer coefficient for the two runs during the morning and afternoon, the time at which the Richardson number reaches its lowest values and consequently the heat transfer coefficient reaches its highest values. Both graphs in Fig. 6 indicate that the heat transfer coefficient is consistently larger in the minimum snow cover run, at the times at which turbulence and mixing most frequently occurs.

This is further verified in Table 6, which lists the important individual energy terms for the two grid points, averaged for the whole month. The latent and sensible heat terms are significantly larger in the minimum snow cover run. These two terms are large enough to cancel the initial large energy difference between the two runs due to the large spread in solar radiation absorbed at the surface so that at these grid boxes, the net heating is equal to or greater in the maximum snow cover run than in the minimum snow cover run. This is the same result obtained for the latitudinally averaged energy balance. Therefore, the processes affecting the energy balance at the two specified grid boxes are applicable to the latitude as a whole.

f. Heat capacity

To determine the magnitude of ΔT produced by any differences in the net heating, it is necessary to know the heat capacity of the first ground layer. After the heat capacity is properly calculated, the latitudinally averaged change in temperature can be computed by dividing the latitudinally averaged change in energy by the latitudinally averaged heat capacity for the first ground layer. The total heat capacity of the first ground layer is

$$\text{heat capacity} = m_e c_{p_e} + m_w c_{p_w} + m_{s+i} c_{p_i},$$

where

- m_e mass of the first ground layer
- c_{p_e} specific heat of dry earth
- m_w mass of water
- c_{p_w} specific heat of water
- m_{s+i} mass of snow and ice
- c_{p_i} specific heat of ice.

At 51°N the numerical value of the heat capacity terms are:

$$m_e c_{p_e} = 0.10 \times 1129950 \text{ J m}^{-2} \text{ K}^{-1}$$

$$m_w c_{p_w} = 5 \times 4218 \text{ J m}^{-2} \text{ K}^{-1}$$

$$m_{s+i} c_{p_i} = (15 + 52) \times 2106 \text{ J m}^{-2} \text{ K}^{-1}.$$

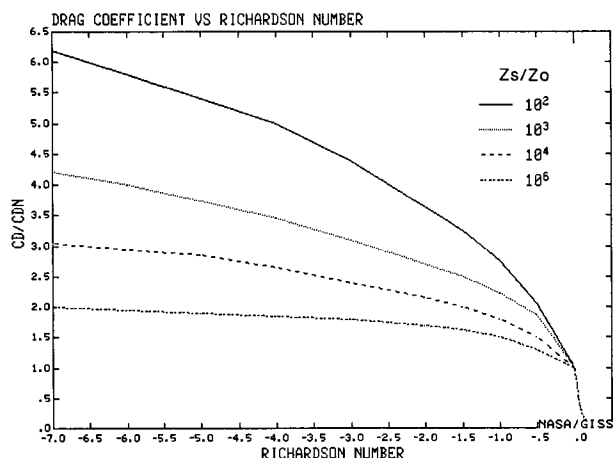


FIG. 5. Richardson number plotted as a function of drag coefficient divided by the neutral drag coefficient (when the Richardson number is equal to zero). Four different values of the surface roughness, z_0 , are shown (actually graphed as a function of the height of the surface layer divided by the surface roughness, z_s/z_0).

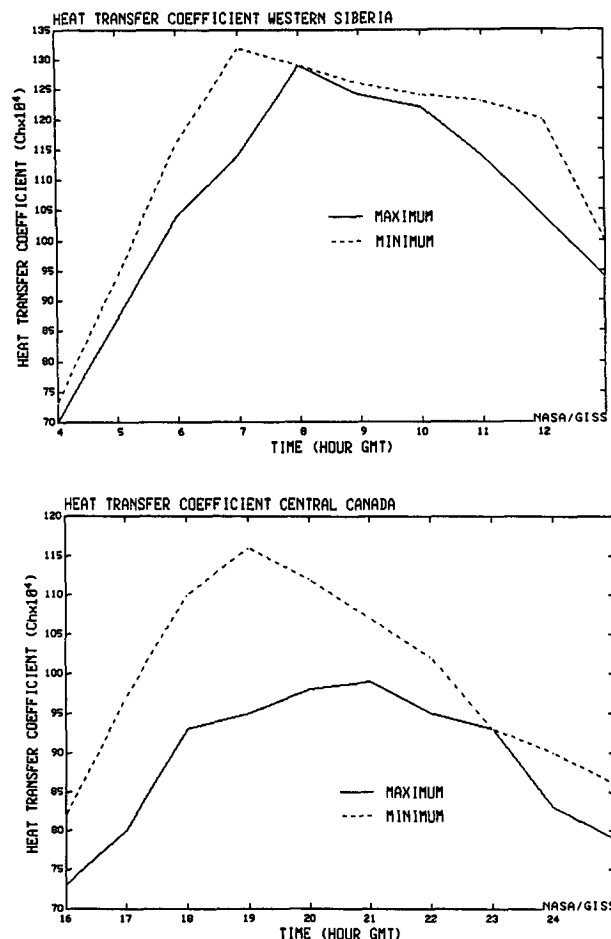


FIG. 6. The five-year monthly averaged hourly values of the heat transfer coefficient C_h , whose dimensions are $\text{W m}^{-2} \text{K}^{-1}$, (the values plotted are the actual values multiplied by 10^4), during the morning and afternoon for (a) western Siberia and (b) central Canada. Plotted are both the maximum snow cover run (solid line) and the minimum snow cover run (dashed line).

For 51°N , a 1 W m^{-2} change, averaged over the entire month would result in a temperature increase of 9.7°C . Therefore, at 51°N latitude (Table 3) the temperature in the maximum snow cover run should be on the order of 20°C warmer than in the minimum snow cover run and not 0.7°C colder as observed.

In the energy balance diagnostic, the latent heat term does not include the latent heat of melting; therefore, the net heating term does not include the loss of energy produced by any snow melted in a particular grid box (in the rest of the paper, whenever the term net heating will be discussed, it will exclude any cooling due to snow melt) and therefore the positive net heating difference is misleading. In the GCM, snow can only melt once the temperature of the ground reaches 0°C , and the temperature of the ground cannot rise above freezing if any snow still exists. Therefore, the net heating

difference of $+2.0 \text{ W m}^{-2}$ at 51°N , between the maximum snow cover run and the minimum snow cover run, would first melt any snow before raising the ground temperature, if the ground temperature were at 0°C . The energy required to melt m mass of snow is

$$\Delta E = mL$$

where L is the latent heat of melting for water. One W m^2 of heating applied over the entire month ($=2\,678\,400 \text{ J m}^{-2}$) would melt $\sim 8 \text{ kg m}^{-2}$ of snow. So for example, for the month of March 1979, the grid box 51°N , 70°E showed a net heating gain of 3.5 W m^2 . Also during the month of March of 1979, the entire snow cover of 44 kg m^{-2} at grid point 51°N , 70°E disappeared. However, not all the snow melts in the model; a significant portion is evaporated directly from the frozen state. The energy of vaporization is included in the latent heat term discussed in the general energy equation for the first ground layer. Therefore, any energy loss due to additional snow that evaporated in the maximum snow cover run is included in the net heating difference of 3.5 W m^{-2} but not energy loss due to snow melt. If it is assumed that one-fourth of the snow cover evaporates and three-fourths melts then $\sim 11 \text{ kg m}^{-2}$ of snow was evaporated and $\sim 33 \text{ kg m}^{-2}$ was melted. To melt 33 kg m^{-2} of snow requires about 4 W m^{-2} of energy. Therefore, after the energy to melt snow is included into the ground's energy balance, the difference in the net heating between the maximum

TABLE 6. The five year averaged energy terms (W m^{-2}) for both the maximum snow cover run and the minimum snow cover run for a) Western Siberia and b) Central Canada. Also included are the net heating term and the temperature of model's first ground layer. All energy terms are rounded off in the tables.

	Snow cover	
	Maximum	Minimum
(a) Western Siberia		
Shortwave radiation	72	98
Longwave radiation	-31	-39
Sensible heat flux	-18	-29
Latent heat flux	-19	-28
Net heating	3	2
Ground temperature ($^\circ\text{C}$)	-8.8	-3.4
(b) Central Canada		
Shortwave radiation	75	87
Longwave radiation	-26	-32
Sensible heat flux	-13	-17
Latent heat flux	-20	-30
Net heating	16	8
Ground temperature ($^\circ\text{C}$)	-3	-2.4

snow cover run and the minimum snow cover run is around -0.5 W m^{-2} . An overall difference of 0.5 W m^{-2} would then account for the -5.4°C difference in temperature between the two runs incurred during March. Similarly, in the maximum snow cover run at 51°N , an overall positive net heating difference can result in cooler temperatures if there was an even greater energy loss due to snow melt.

g. Five-day experimental runs

In the last part of the experiment, three years were chosen in which model runs were conducted for every five days of the month of March (1978, 1979, 1980), i.e., the model was run for five days at a time and diagnostics were generated at the end of the fifth day that contained five-day averages of the hourly diag-

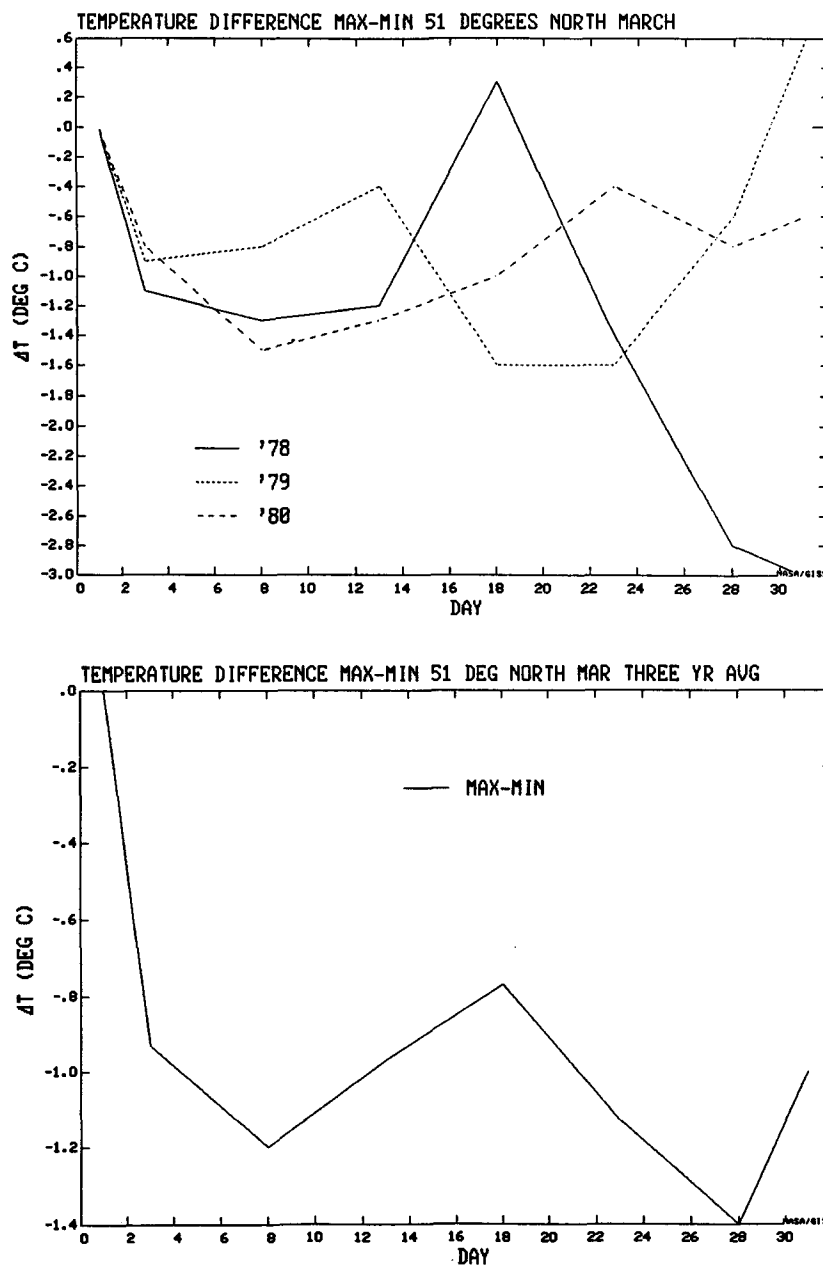


FIG. 7. The five-day averaged temperature difference, at 51°N , plotted over the course of the month of March. (a) Three different years are shown, March 1978 (solid line), March 1979 (dotted line) and March 1980 (dashed line). (b) The average of all three years.

nostics. The purpose of breaking down the month into five-day intervals was to record the trend of the energy and temperature values during the course of the month.

The graph of the temperature difference, ΔT , between the maximum snow cover run and the minimum snow cover run, is presented in Fig. 7 for each individual year. Also shown is the three-year average. In all three years, the first few days are characterized by a quick drop in temperature, which is on the order of 1°C . After this period, the temperature difference decreases through the second week (in March 1978 it even becomes positive). During the second half of the month a negative temperature difference is also recorded, but embedded in the trend are oscillations that appear to be randomly generated, and no set pattern can be determined. Before any explanation can be given as to why the temperature trend behaves as it does throughout the month, the energy term differences must be explored since the temperature trend is a direct result of the sum of all the diabatic heating terms.

Figure 8 is the plot of the energy term differences between the maximum snow cover run and the minimum snow cover run. Also included is the difference in snow melt between the two runs, converted into equivalent energy units. For all three years, the first two and one-half weeks produced qualitatively the same result. By far, the two most dominating energy terms in the energy balance difference are the solar radiation term, and the combined sensible and latent

heat terms. Within the first few days, the maximum snow cover model run accrues a large solar radiation deficit. The initial cooling associated with the solar radiation decrease results in changes to the sensible and latent heat fluxes. These changes are exactly opposite to the solar radiation changes, the maximum snow cover run gains a large amount of energy through the sensible and latent heat terms relative to the minimum snow cover run (i.e., the sensible and latent heat fluxes are not as large heat sinks in the maximum snow cover run as in the minimum snow cover run). The gain from the sensible and latent heat terms is ultimately as large as the energy lost from the reflected solar radiation.

The difference in the energy contribution from the longwave radiation and the snow melt is almost an order of magnitude smaller than the other energy terms. Again, for the first half of the month the contribution from these two terms is steady; i.e., the longwave radiation shows a slight gain of energy in the maximum snow cover run, and the snow melt term shows an energy deficit in the maximum snow cover run.

After the first half of the month, the difference between the two runs in the solar radiation term and in the snow melt term continues to be negative when summed over the entire period. During the same time period, the difference in the sensible and latent heat terms and in the longwave radiation term continue to record a net gain. As found in the temperature curves,

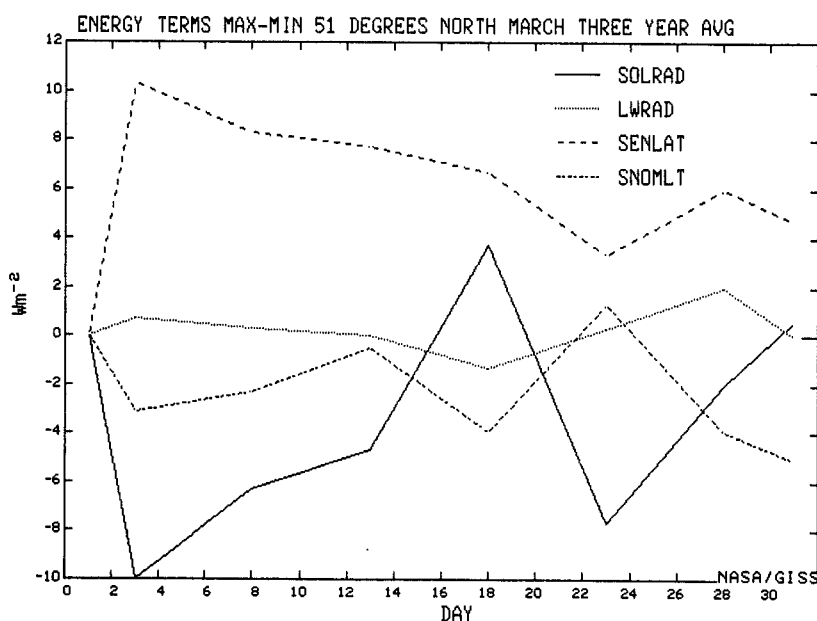


FIG. 8. Latitudinally averaged, five-day-averaged differences of the following energy terms: the absorbed solar radiation (solid line), the emitted longwave radiation (dotted line), the combined sensible and latent heat (dashed line) and the snow melt converted into equivalent energy units (uneven dashed line), averaged for March 1978, 1979, and 1980 at 51°N .

oscillations are embedded in the energy term curves, a result of the synoptic forcings. At the beginning of the month, the snow is relatively fresh and deep so that any forcings due to the snow cover can easily manifest themselves in the energy trends, despite the synoptic situation. As the month progresses, the snow ages and melts. The forcings due to snow cover become weaker and more diluted so that increasingly throughout the month, the synoptic forcings become of greater importance in the trend of the energy terms.

In Fig. 9 the difference in the net heating is plotted together with the difference in the snow melt term. The net heating difference term is a summation of the following terms: the solar radiation term, the longwave radiation term, the sensible heat term, the latent heat term and the precipitation heat term. With the exception of some brief periods, the net heating difference between the maximum snow cover run and the minimum snow cover run, in all three months, was positive, in contrast to expectation. The net heating difference and the snow melt difference are negatively correlated throughout the month, i.e., the more the net heating is positive the more the snow melts and thus becomes a larger sink of energy. Without the excess net heating at the surface, the snow cover would have perpetuated itself, as is sometimes assumed.

Thus, while the snow cover did cause a significant energy deficit at the surface due to the increased amount of solar radiation reflected away, the snow cover ultimately caused the surface to gain energy in

excess of the solar radiation that was lost. This is mainly due to the inability of the surface to lose energy in the form of sensible and latent heat, energy that would have been lost had the snow cover not been present. Therefore, the snow cover produces a positive heating, which would normally raise the surface temperature. However, because snow cover is present, the temperature cannot rise above 0°C and any additional heating melts the snow instead.

h. January run

It is thought that the cooling effect of snow cover on surface temperatures is maximized during late winter. The incoming solar radiation is substantially more in mid- to late March than early to mid-January. Therefore, the absolute amount of shortwave radiation reflected by the high albedo of snow cover increases significantly as winter progresses. For this reason our experiment was conducted during the month of March.

However, it is possible that this reasoning is faulty. With the larger amounts of incoming solar radiation and the large negative feedbacks produced in our experiment, anomalous snow cover is removed more effectively than it would be earlier in the winter. Maximum cooling due to snow cover may be realized during the early to mid-winter time period when the anomalous snow cover, and its influence on surface temperatures, can persist for longer periods.

In order to test this hypothesis, a maximum and a

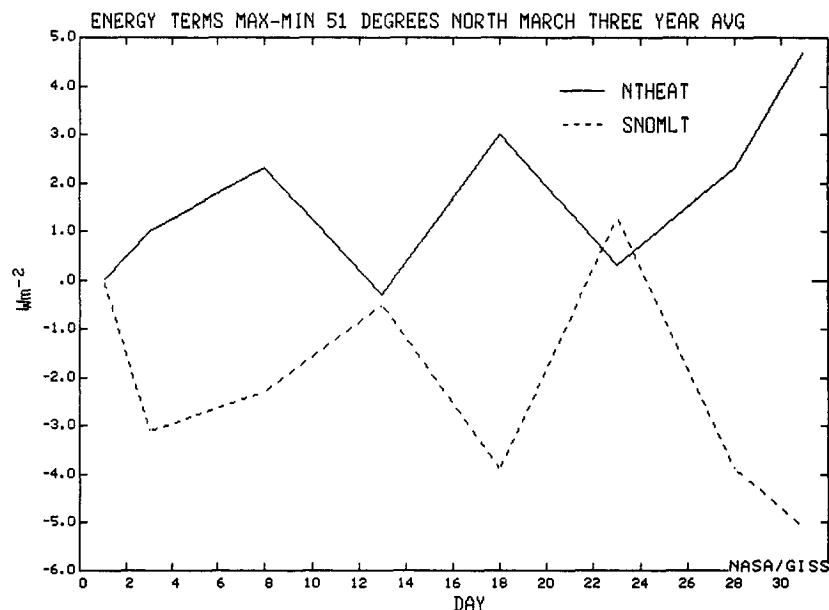


FIG. 9. Latitudinally averaged, five-day-averaged differences for the net heating term (solid line) and the snow melt term (dashed line) averaged for all three years at 51°N . The net heating term is the summation of the absorbed solar radiation, emitted longwave radiation, the sensible heat flux, the latent heat flux and the precipitation heat flux.

minimum snow cover run were repeated for the month of January. However, given the nature of these experiments, the model is free to alter its snow cover away from the initial conditions, and it progressively adds snow cover in the minimum snow cover run, reducing the monthly average snow cover differences. Thus, we concentrate on the first week of the experiment, while there is still a large difference in the snow cover between the two runs, and during the time in which the greatest cooling occurred in the March experiments (see Fig. 7).

The results are shown in Table 7. With similar snow cover differences, the January and March results provide similar net cooling between the maximum and minimum snow cover situations. The energy terms in January are all reduced, but similar balances apply: the reduction in shortwave radiation in the maximum snow cover run is more than balanced by the reduced energy losses, and its net heating is increased by 2 W m⁻² for both times of year. The overall negative net heating in January does allow the snow cover to remain longer (note the higher snow coverage percentage in January), but the reduced solar radiation (the reason the snow can stay longer) means that the presence of the snow cover has less effect on the net solar radiation absorbed at the surface. At least on the weekly time scale, these compensating effects make the impact of snow cover on temperatures relatively independent of the winter month chosen. Given that even in March

substantial snow was present for the whole month at this latitude (snow cover averaged 67% for the entire month in the maximum snow cover run), the monthly time-scale differences should show a similar insensitivity.

4. Discussion

Any comprehensive conclusions about the effects of snow cover on the surface temperature and the energy balance must include the influence of snow cover on all the diabatic heating terms, rather than focusing on just one of the terms. There seems to be a very definite cycle forced on the energy balance by the presence of snow cover, and similar to many other forcing mechanisms found in nature, there seems to be a negative feedback built into it. The energy terms can be divided into two groups depending on what role the different energy terms play within this negative feedback cycle. The criteria for which energy term gets classified into which group is based on the relationship between the individual energy term and the surface temperature. The first group of energy terms are directly influenced by the physical properties of snow cover, its high albedo and its large latent heat of melting. Both of these properties of snow cover contribute a negative gain of energy in the net heating. This effect of snow cover causes a significant cooling in the surface temperature. This first group of energy terms is labeled the "action" energy terms because they directly act on the surface temperature.

The second group of energy terms is indirectly affected by the snow cover. These terms are not altered so much by the physical properties of snow cover as they are by the impact of snow cover on the environment. This second group of energy terms is labeled the "reaction" energy terms because they react to the temperature change induced by the snow cover. This second group consists of the emitted longwave radiation, and the sensible and latent heat flux.

It is because of this second group of energy terms that the feedback cycle produced by the snow cover is a negative one. The atmosphere has its own properties by which it can react to temperature anomalies being forced upon it: the vertical transfer of energy and mass is dependent on the vertical temperature profile. The increased stability, caused by the cooling, quickly suppresses the flux of sensible and latent heat away from the surface. The gain in the net heating is large enough to reverse the negative heating trend occurring at the surface. In its stead, an overall positive heating term (not including snow melt) is produced the remainder of the time that the anomalous snow cover remains. So in the case of an anomalous snow cover, the anomaly will work to eventually extirpate itself rather than to perpetuate itself.

TABLE 7. The energy terms for both the maximum snow cover run and the minimum snow cover run for the first five days of (a) January 1979 and (b) March 1979 at 51°N. Also included are the net heating term, the temperature of model's first ground layer and snow cover (percentage).

	Snow cover	
	Maximum	Minimum
(a) 1-5 January 1979		
Shortwave radiation	22	26
Longwave radiation	-23	-25
Sensible heat flux	0	-2
Latent heat flux	-3	-4
Precipitation heat flux	-3	-3
Net heating	-7	-9
Ground temperature (°C)	-9.8	-9.2
Snow cover (%)	85	64
(b) 1-5 March 1979		
Shortwave radiation	73	81
Longwave radiation	-36	-36
Sensible heat flux	-9	-12
Latent heat flux	-24	-32
Precipitation heat flux	-4	-4
Net heating	0	-2
Ground temperature (°C)	-6.3	-5.4
Snow cover (%)	74	53

Three stages are proposed for this cycle based on which group of energy terms plays the dominant role for the duration of that particular stage of the cycle. The beginning and the end of the cycle are determined by the sign of the slope of the net heating difference curve (this includes snow melt).

1) Stage I: the "action" stage during which the maximum snow cover run cools relative to the minimum snow cover run with respect to time.

2) Stage II: the "reaction" stage when a reversal takes place in the heating trend and the maximum snow cover run warms relative to the minimum snow cover run with respect to time.

3) Stage III: the final stage wherein the difference in net heating oscillates around zero, in a seemingly random and natural mode.

The nature of the three stages is such that if the derivative of the difference in the net heating were plotted versus time, the curve would resemble a negative sine curve.

The first stage is characterized by the net heating difference between the two runs becoming increasingly negative. The maximum snow cover run cools relative to the minimum snow cover run as a response to the energy sinks created by the presence of snow cover: the high albedo and the snow melt. With all the other energy terms responding more slowly to the presence of snow cover, a cooling trend commences.

It is the nature of this cooling trend, however, which causes Stage I to transform into Stage II within a relatively short period of time. The cooling is not uniform throughout the atmosphere, instead it is confined to a very shallow layer at the surface. Cooling the atmosphere only near the surface increases the stability of the atmosphere. The greater stability inhibits energy, in the form of sensible and latent heat, from being transported away from the surface. In addition, and to a lesser extent, the lower temperatures reduce the amount of longwave radiation emitted by the surface. As the cooling continues to increase, the surface becomes more ineffective at ridding itself of sensible heat, latent heat, and longwave radiation. Shortly thereafter, enough heat is trapped at the surface because of these three terms to reverse the cooling trend. Stage II is characterized by the maximum snow cover run gaining heat, or warming, relative to the minimum snow cover run.

The third stage, which can be categorized as an energy stalemate, is simply a consequence of the snow melting and aging. As the snow ages and melts, its primary influence on the energy budget, its high albedo, begins to wane (refer back to Fig. 8). As less and less energy is being lost due to the reflection off the snow cover, also lost is the forcing that the snow cover exhibits on the energy balance. As a further consequence, less and less energy is supplied from the sensible and

latent heat terms to counterbalance the cooling that resulted from the high albedo. Even though energy is still being lost through snow melt, it is generally less significant than the energy lost due to the high albedo of snow cover (with the possible exception of a rapid melt-off of a deep snow cover). The weaker the forcings produced by the snow cover, the more important become the randomly generated synoptic forcings. Without any of the energy terms driving the net heating in any organized direction the difference in the net heating simply oscillates in a natural mode. The trend of the net heating for the month of March and how it is subdivided among the stages is presented in Fig. 10.

The net result of all three stages is to produce a slight cooling over a large area, on the order of 1°C . For example, the latitudinally averaged cooling at 51°N is 0.7°C for the month of March. However, locally the cooling can be much larger, especially in continental regions. In our experiment the largest cooling produced was 6°C in one grid box in central Siberia. It is even possible that a finer resolution model could produce locally, cooling of even greater magnitude. Even so, these results differ substantially from some of the empirical studies noted in the Introduction. How can this discrepancy be explained? Obviously the model may be underestimating the snow cover impact for some reason, perhaps associated with its boundary layer physics. Even so, it is important to note that serious questions remain associated with the empirical studies.

The empirical studies themselves have not been consistent; for example, Walsh et al. (1982) found a 5° – 7°C cooling, while Walsh et al. (1985) found only a 1° – 2°C cooling. The latter result is certainly consistent with the modeling study reported here. At the basis of these ambiguities lies a fundamental difficulty: it is hard to separate the thermodynamic effect of snow cover from the dynamical influence of the regime which produced the snow cover.

Attempts have been made to separate these two influences by relating the 700 mb height field to surface temperatures with and without the presence of snow cover. In one such example, Namias (1962) concluded that the snow cover induced cooling up through 700 mb. As the 700 mb height is related to the surface pressure and the mean temperature of the air column below, then in this example the surface pressure must have been higher with snow cover present. But was this higher pressure the result of snow cover or was it associated with stronger cold air advection, which then helped to produce the observed cooling? The question cannot be answered empirically and requires modeling studies.

5. Conclusion

Accepted theory predicts that snow cover causes a significant cooling in the surface temperatures. Snow

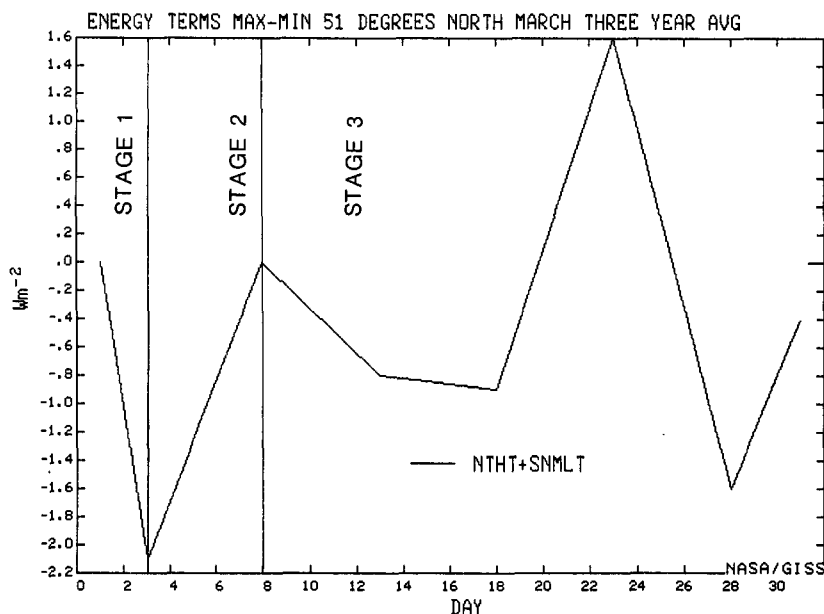


FIG. 10. The three-year-averaged, five-day-averaged net heating difference term during the month of March for 51°N. The curve is divided into three sections to illustrate how the three stages, proposed in the text, are divided along the net heating difference curve. The first line demarcates the end of the first stage, the second line demarcates the end of the second stage, and the remainder of the month is the third stage.

cover has been attributed with modifying the earth's energy balance by lowering the shortwave radiation absorbed at the surface and increasing the longwave radiation emitted by the surface, factors that would combine to produce lower temperatures over snow covered surfaces as compared to non-snow covered surfaces. Therefore, in a given locality, a positive feedback would be set up between positive anomalous snow cover and negative anomalous temperatures, i.e., one will reinforce the other.

Most of the prior studies conducted to verify this relationship, have been empirical in nature. In these studies, it was assumed that snow cover was the independent variable and temperature was the dependent variable. However in fact, snow cover is also dependent on temperature, and both snow cover and temperature are dependent on the circulation. Modeling studies have not concentrated on these interactions, and in the most sophisticated modeling experiment completed to date, the negative feedback between snow cover and net heating is similar to that reported here (Barnett et al. 1988). Studies done with models that do not include stability-dependent turbulence parameters (e.g., NCAR CCM, refer to Holloway and Manabe 1971) will miss this important feedback process and may overestimate the snow impact.

In the experiment reported here, the effect of snow cover on temperatures is explored with two experimental runs: one with an extensive snow cover and one with a sparse snow cover. The synoptic situations

in both runs were initially identical, except for the modifications forced solely by the presence or absence of snow cover. In this way, the dependence of snow cover and temperatures on an independent general circulation was minimized by taking the difference between the two model runs.

The results of the GCM experiment emphasize the strong negative feedbacks which limit the duration of the influence of snow cover. When comparing the maximum snow covered run to the minimum snow covered run, only the absorbed shortwave radiation term necessarily contributes to lower temperatures. Even though the cooling is significant, the order of magnitude is much less than expected from the differences in the ground albedo caused by the snow cover. The resultant cooling is better correlated with changes in the planetary albedo, which shows much smaller differences than those differences in the ground albedo. Furthermore, in contrast to current theories, if melting snow is not included all the remaining heating terms contribute to increasing the net heating over a snow covered surface. Only after the latent heat of melting snow is included in the overall heating, does the energy balance at the surface become negative. Therefore, anomalous snow cover acts to remove itself, rather than to perpetuate its existence as has heretofore been assumed.

The results of the modeling experiment indicate that because the cooling is confined to a shallow layer it stabilizes the atmosphere, inhibiting sensible and latent

heat transport away from the surface. When snow cover is present, the reduced sensible and latent heat flux terms contribute to a positive heating on the same order of magnitude as the cooling from the shortwave energy term. This response by the sensible and latent heat terms nearly nullifies any cooling due to the high albedo of snow cover. Therefore, a positive feedback between above-normal snow cover and below-normal temperatures does not materialize and on time scales of greater than a week, the cooling realized is slight.

Acknowledgments. We would like to thank Reto Reudy and Bob Suozzo for helping with model runs and Dr. Anthony Del-Genio, Cynthia Rosenzweig, James Foster and Dorothy Hall for useful comments and suggestions. Climate modeling at GISS is supported by the NASA Climate Program Office.

REFERENCES

- Barnett, T. P., L. Dumenil, U. Schlese and E. Roeckner, 1988: The effect of Eurasian snow cover on global climate. *Science*, **239**, 504–507.
- , —, —, — and M. Latif, 1989: The effect of Eurasian snow cover on global climate variations. *J. Atmos. Sci.*, **46**, 661–685.
- Deardoff, J. W., 1967: Empirical dependence of the eddy coefficient for heat upon stability above the lowest 50 m. *J. Appl. Meteor.*, **6**, 631–643.
- Dewey, K. F., 1977: Daily maximum and minimum temperature forecasts and the influence of snow cover. *Mon. Wea. Rev.*, **105**, 1594–1597.
- Foster, J., M. Owe and A. Rango, 1982: Snow cover and temperature relationships in North America and Eurasia. *J. Climate Appl. Meteor.*, **22**, 460–469.
- Hansen, J., G. Russell, D. Rind, P. Stone, A. Lacis, S. Lebedeff and L. Travis, 1983: Efficient three dimensional global models for climate studies: Models I and II. *Mon. Wea. Rev.*, **111**, 609–662.
- Holloway, J. L. Jr. and S. Manabe, 1971: Simulation of climate by a global general circulation model. I: Hydrologic and heat balance. *Mon. Wea. Rev.*, **99**, 335–370.
- Klein, W. H., 1983: Objective Specification of monthly mean surface temperatures in the United States during the winter season. *Mon. Wea. Rev.*, **111**, 674–691.
- , 1985: Space and time variations in specifying monthly mean surface temperature from the 700 mb height field. *Mon. Wea. Rev.*, **113**, 277–290.
- , and J. E. Walsh, 1983: A comparison of pointwise screening and empirical orthogonal functions in specifying monthly mean surface temperature from 700 mb data. *Mon. Wea. Rev.*, **111**, 669–673.
- Kukla, G., 1979: Climate role of snow covers. *Sea Level, Ice, and Climate Change*, 79–107.
- Matson, M., C. F. Ropelewski and M. S. Varnadore, 1986: *An Atlas of Satellite-Derived Northern Hemisphere Snow Cover Frequency*, NOAA Atlas, U.S. Govt. Printing Office: 1986-151-384, 75 pp. [Copies Available from NOAA/NESDIS (E/RA22), 5200 Auth Road, Wash. D.C. 20233.]
- Meehl, G. A., and W. M. Washington, 1988: A comparison of soil moisture sensitivity in two global climate models. *J. Atmos. Sci.*, **45**, 1476–1492.
- Namias, J., 1960: Snowfall over eastern United States: Factors leading to its monthly and seasonal variations. *Weatherwise*, **13**, 238–247.
- , 1962: Influences of abnormal heat sources and sinks on atmospheric behavior. *Proc. Int. Symp. on Numerical Weather Prediction*, Tokyo, Meteor. Soc. Japan, 615–627.
- , 1985: Some empirical evidence for the influence of snow cover on temperature and precipitation. *Mon. Wea. Rev.*, **113**, 1542–1553.
- Petersen, R. A., and J. E. Hoke, 1989: The effect of snow cover on the regional analysis and forecast system (RAFS) low-level forecasts. *Wea. Forecasting*, **4**, 253–257.
- Rind, D., D. Peteet and G. Kukla, 1989: Can Milankovitch orbital variations initiate the growth of ice sheets in a general circulation model? *J. Geophys. Res.*, **94**, 12 851–12 871.
- Robinson, M., and R. Bauer, 1981: Oceanographic Monthly Summary, 1, No. 2, NOAA National Weather Service, W322, Washington, DC, pp. 2–3.
- Robock, A., 1980: The seasonal cycle of snow cover, sea ice and surface albedo. *Mon. Wea. Rev.*, **108**, 267–285.
- Rossow, W. B., and A. A. Lacis, 1990: Global, seasonal cloud variations from satellite radiance measurements. Part II: Cloud properties and radiative effects. *J. Climate*, **3**, 1204–1253.
- Sellers, W. D., 1965: *Physical Climatology*. The University of Chicago Press, 272 pp.
- Wagner, A. J., 1973: The influence of average snow depth on monthly mean temperature anomaly. *Mon. Wea. Rev.*, **101**, 624–626.
- Walsh, J. E., 1984: Snow cover and atmospheric variability. *Amer. Sci.*, **72**, 50–57.
- , and B. Ross, 1986: Synoptic scale influences of snow cover and sea ice. *Mon. Wea. Rev.*, **114**, 1795–1810.
- , and —, 1988: Sensitivity of 30 day dynamical forecasts to continental snow cover. *J. Climate*, **1**, 739–754.
- , D. R. Tucek and M. R. Peterson, 1982: Seasonal snow cover and short term climatic fluctuations over the United States. *Mon. Wea. Rev.*, **110**, 1474–1485.
- , W. H. Jaspersion and B. Ross, 1985: Influences of snow cover and soil moisture on monthly air temperature. *Mon. Wea. Rev.*, **113**, 756–769.